We are IntechOpen, the world's leading publisher of Open Access books Built by scientists, for scientists

6,900
Open access books available

185,000
International authors and editors

200M
Downloads

Our authors are among the

154
Countries delivered to

TOP 1%
most cited scientists

12.2%
Contributors from top 500 universities

WEB OF SCIENCE™

Selection of our books indexed in the Book Citation Index in Web of Science™ Core Collection (BKCI)

Interested in publishing with us?
Contact book.department@intechopen.com

Numbers displayed above are based on latest data collected.
For more information visit www.intechopen.com

13

MicroCT: An Essential Tool in Bone Metastasis Research

Bethany A. Kerr and Tatiana V. Byzova
Lerner Research Institute, The Cleveland Clinic
United States of America

1. Introduction

Microcomputed tomography (microCT) is an essential tool for the study of small animal osseous and soft tissue structures. While several other technologies can be used to image bone, vasculature, and other soft tissues, microCT alone provides high spatial resolution of both hard and soft tissues. Prior to the development of microCT imagers, small animal research was conducted in clinical CT scanners; however, a consequence was poor resolution of the smaller tissues. The development of microCT permitted enhanced small animal imaging resolution and increased use of microCT in preclinical studies. Recent improvements to X-ray detector sensitivity have resulted in the ability of microCT, in combination with contrast agents, to be used in soft tissue studies. In clinical scanning, barium or iodine are typically used for soft tissue assessment; while in small animals, intraperitoneal injections of non-ionic water-soluble contrast medium or intravenous injections of a barium/gelatin mixture can be used for the visualization of soft tissues and vasculature (Paulus et al., 2000). This chapter will focus on the use of microCT to scan osseous tissues. The use of microCT has been well characterized in the study of bone development, fracture repair, biomaterial integration, osteoporosis, and, more recently, cancer bone metastasis.

MicroCT allows for the creation of three-dimensional images of the bone which can be processed both qualitatively and quantitatively. MicroCT analysis quantifies several bone structural indices: bone mineral density (BMD), bone volume to total volume ratio (BV/TV), bone surface area (BSA), trabecular number (Tb.N), trabecular thickness (Tb.Th), and trabecular spacing (Tb.Sp). In addition, since microCT is non-destructive, the same specimens can then be used for mechanical testing, histological analysis, or further experiments. MicroCT scanning is the ideal method for assessing bone structure compared with magnetic resonance imaging (MRI), positron emission tomography (PET), X-rays, or bone histomorphometry (Table 1).

Magnetic resonance imaging (MRI) is non-ionizing and ideal for soft tissue scanning, but not for osseous tissue. Although overall changes in the bone architecture can be seen, MRI cannot provide a structural analysis of bone tissue (Jiang et al., 2000). In addition, small animal MRI devices have micrometer spatial resolution, similar to microCT, but low sensitivity compared with highly sensitive microCT (Mayer-Kuckuk & Boskey, 2006). Overall, MRI has been used extensively for bone research and can provide some information on the bone structure and its level of mineralization, but is not as quantitative as microCT

scanning. Finally, microCT scanners for small animals are considerably smaller and less expensive than MRI machines.

Parameter	MicroCT	MRI	PET	X-ray	Histomorphometry
Small animal	Yes	Yes	Yes	Yes	Yes
Sensitivity	High	Low	High	Low	N/A
Spatial Resolution	Micrometer	Micrometer	Millimeter	Millimeter	Micrometer
Structural Quantification	Yes	Minimal	No	Minimal	Yes
Mineralization Levels	Yes	Yes	No	Minimal	Yes
Non-destructive	Yes	Yes	Yes	Yes	No

Table 1. Comparison of imaging technologies for assessing bone structure. MicroCT: microcomputed tomography, MRI: magnetic resonance imaging, PET: positron emission tomography.

Positron emission tomography (PET) is useful for functional imaging and gene expression studies; however, it requires the use of radiolabeling. Single photon emission computed tomography (SPECT) also requires the use of isotopes, but has improved resolution compared with PET. Small animal PET and SPECT have high sensitivity and easy signal quantification, but cannot provide anatomical information and thus are not as effective in assessing the bone structure and mineralization as microCT. In addition, the spatial resolution of PET is at the millimeter level, which is very low for imaging small animals and thus does not provide as detailed a picture of the bone structure in small animals compared with microCT (Mayer-Kuckuk & Boskey, 2006; Paulus et al., 2001). Thus, while PET and SPECT are sensitive imaging methods, their use of isotopes and low spatial resolution prevent these imaging methods from being ideal choices for studying the bone architecture.

x-ray technology provides a two-dimensional image of the bone structure. While bone mineralization is often measured by X-ray, the accuracy of measurements is much greater using microCT. For example, a larger change in BMD must occur to be measured by x-ray, compared with microCT. In fact, microCT scanning can measure a change in cortical thickness of 10-20% which would be undetectable using x-ray imaging. In addition, microCT can distinguish between fractured and non-fractured vertebrae better than x-rays (Genant et al., 2008). Further, while radiography can indicate a loss of mineral, only microCT can differentiate between a thin layer of highly mineralized tissue and a thick layer of less mineralized tissue (Gielkens et al., 2008). Additionally, microCT analysis allows for the cortical and trabecular bone to be analyzed separately, which cannot be done with x-rays (Ravoori et al., 2010). Thus, microCT analysis presents a complete picture of the bone structure, which cannot be accomplished using x-rays.

Quantitative bone morphometry originally was determined from two-dimensional bone biopsies and used to measure structural indices of the bone. MicroCT allows for three-dimensional measurements of a majority of the same structural indices. Bone volume density and bone surface density can be measured equally well by histomorphometry and microCT. However, only microCT can accurately measure Tb.Th, Tb.Sp, and Tb.N, which

must be assumed using "ideal" plates and rods in histomorphometry (Muller, 2009). Further, microCT detects bone loss earlier than histomorphometry (Laib et al., 2000). An advantage of histomorphometry is the evaluation on a cellular level (Gielkens et al., 2008); however advances in microCT are improving resolution to the cellular level and negating this advantage.

2. A history of microCT in bone research

The advantages of microCT scanning over other methods have resulted in improved qualitative and quantitative analysis of small animal bone structure leading to the increased prevalence and utilization of microCT to study the bone structure over the past decade. Quantitative microCT measurements are highly reproducible in both rats and mice (Nishiyama et al., 2010). This reproducibility, in combination with the availability of transgenic animals, has led to important studies elucidating the mechanisms of various proteins and genes controlling bone development, bone healing, osseointegration, osteoporosis, and the progression of primary and metastatic bone cancers.

2.1 MicroCT bone research applications

Most orthopaedic research examines the development, maintenance, and repair of skeletal tissues and utilizes microCT scanning for structural analysis during these processes. MicroCT scanning relies on the mineralization of bone to detect the bone architecture and thus cannot be used to study cartilage or other soft materials. However, changes in the bone architecture or bone mineralization can be used to describe alterations in bone development, bone healing, biomaterial integration, or osteoporosis. The measurement of these changes by microCT allows for the development of therapeutics and an understanding of the molecular mechanisms governing these processes.

2.1.1 Bone development

Bone development occurs through one of two processes: intramembranous or endochondral ossification. Endochondral ossification is the development method of the long bones, during which a cartilaginous anlagen is remodelled and replaced by bone, while intramembranous ossification is used predominantly by the skull. The process of bone development and the genes and proteins involved have been extensively studied using knock-out mice. Using these transgenic mice, the importance of genes and proteins in controlling the structure and mineralization of the skeleton produced by intramembranous or endochondral ossification can be studied using microCT analysis. MicroCT analysis permits quantification of developmental delays in the formation of bones throughout the body in response to changes in developmental cues. In addition, the progression and genetic etiology of osteogenesis imperfecta, a genetic disorder of fragile bones, can be studied by microCT scanning. Using various genetically altered mice, the developmental changes resulting in osteogenesis imperfecta have been elucidated. In addition, possible interventions and treatments for the disease can be tested using microCT to measure changes in mineralization. Thus using microCT scanning and genetically altered mice, factors controlling bone mineralization, skull and vertebral development, and developmental bone architecture have been elucidated.

2.1.2 Bone healing and fracture repair

After a bone fracture, a non-union space is often left, which must be healed through a proliferative process, part of which can be visualized by microCT imaging. The distance between the bones and the angle of fracture govern the speed of healing and both of these parameters can be measured shortly after fracture by microCT. During the healing process, the first, reactive phase is marked by increased inflammation and granulation tissue formation. In the second, reparative phase, chondrocytes and osteoblasts migrate into the gap. Chondrocytes begin to lay down a cartilaginous callus, which is then mineralized by osteoblasts producing woven bone through endochondral ossification, which recapitulates bone development. In the final, remodelling phase, osteoblasts and osteoclasts remodel the woven bone into cortical and trabecular bone with a similar shape and mechanical strength to the original bone. MicroCT imaging can be used during the reparative and remodelling phases to assess the healing process. MicroCT analysis provides information on the temporal and topographical changes which occur as the callus is reorganized into bone and during the final remodelling phase (Freeman et al., 2009). Further, microCT scanning can be used to determine the effectiveness of different treatments and interventions in accelerating or improving the bone healing process. In particular, the use of low-intensity pulsed ultrasound to accelerate fracture healing has been studied extensively using microCT analysis (Freeman et al., 2009). Thus, microCT scanning can be used to assess the fracture healing process and to measure the effectiveness of therapeutics aimed at accelerating the process.

2.1.3 Biomaterial research

The osseointegration of bone tissue with implants and scaffolds is integral to bone regeneration and to prevent loosening, rejection, and microdamage to the bone surrounding the implant which could result in fatigue fractures and catastrophic failures. Scaffolds and implants need to encourage bone growth into the porous portions without the formation of fibrous capsules around the implant, which prevent osseointegration. MicroCT analysis has several functions in the design of scaffolds and implants (Rolf et al., 2010). MicroCT scanning can be used to produce 3D images of the scaffold or implant pores to properly measure the porosity which affects permeability, cell migration and bone ingrowth. In addition, the pore interconnect diameter and number of connections per pore can also be measured. An ideal scaffolding material will have porosity and interconnection size and number similar to that of trabecular bone, which can be compared directly using microCT (Jones et al., 2009). After implantation of an implant or scaffold, the levels of mineralized tissues within the pores over time can be measured using microCT; although this measurement can be difficult if the implant material is similar to the ingrowing bone. Nonetheless, changes in pore size can still be measured and any changes would correlate with bone ingrowth (Jones et al., 2009; Reynolds et al., 2009). In a recent study using titanium foam to coat implants, microCT scanning was used to first measure the differences in porosity of dense titanium and foam covered implants and was then used to measure the amount of bone ingrown into the implant after 2 weeks (Wazen et al., 2010). Further, microCT analysis can be used to diagnose osteomyelitis, which is caused by peri-prostethic infection and is a leading cause of implant rejection. The coating of implants with antibiotics to prevent infection is currently being studied. This implant coating prevents the growth of bacteria after implantation and inhibits the associated bone destruction, which

can be measured non-invasively by microCT (Adams et al., 2009). Thus, microCT analysis can also be used to study the osseointegration of various biomaterials.

2.1.4 Osteoporosis

MicroCT imaging is especially important for the study of osteoporosis, particularly disease progression and treatment efficacy, as it is one of the few imaging techniques which can provide information on the bone mineral content and density. In addition, scanning is non-invasive and images can be registered to assess changes over time (Ruegsegger et al., 1996). For example, microCT has been used to measure changes in BV/TV, Tb.Th, and Tb.N in the iliac crest of human bone biopsy specimens to determine the extent of osteoporosis and the effects of various drug interventions. Additionally, microCT is used to study osteoporosis in small animals. To study the effects of hormones and preclinical treatments, mice and rats undergo ovariectomies and are monitored for changes in the bone structure including decreased trabecular connectivity and decreased BV/TV which can result from decreased hormones (Genant et al., 2008). In addition, the use of estrogen replacement therapy to rescue ovariectomized mice has been measured using microCT and has shown that BV/TV is restored, but that the connectivity of the trabeculae remains decreased (Jiang et al., 2000). To further study osteoporosis prevention, the role of mechanical stress was assessed by subjecting mice to hindlimb unloading by tail suspension for 2 weeks and bone architecture was monitored using microCT scanning. Using this method, mechanical stress was shown to be integral to maintaining the bone structure and density (Martin-Badosa et al., 2003). Using ovariectomies and hindlimb unloading, several therapies and the importance of mechanical stress, representing exercise, have been validated in mouse models leading to improved treatment and prevention of osteoporosis.

2.1.5 Primary bone cancers

Primary bone cancers can be either benign (osteochondromas) or malignant. Malignant bone tumors include chondrosarcomas, Ewing's sarcoma, and osteosarcomas. Although uncommon, these primary bone cancers have a high incidence of recurrence and can be difficult to diagnose. MicroCT density measurements can be used to differentiate between chondrosarcomas and osteosarcomas in patient samples, as chondrosarcomas were found to have a lower density within the tumors compared with osteosarcomas, although the trabecular densities were similar (Langheinrich et al., 2008). Further, since osteosarcomas occur in the bone osteoid, they are most often studied using microCT. In these tumors, microCT scanning is often performed to monitor tumor growth and lesion characteristics. In addition, the presence of further disease progression and the development of metastases can also be determined using repeated microCT scanning (Yang et al., 2007). Thus, microCT imaging can be used to assist in the diagnosis and monitoring of primary bone cancers.

2.1.6 Bone metastasis

Several cancers metastasize to the bone, specifically: breast, kidney, lung, prostate, thyroid, and multiple myelomas. The process of bone metastasis has been primarily studied in breast, myelomas, and prostate cancers, which display preferences for the bone environment in human metastasis. In small animal models, bone metastasis is often studied via the injection of cancer cells intravenously, intracardiacally, orthotopically or intratibially. These injected cells can then colonize the bone and these metastatic tumors are either osteoblastic,

osteolytic, or a combination of both. MicroCT has been used primarily to study changes in the bone microenvironment in response to a metastatic tumor, as discussed in detail in the following section. In some cases, human bone has been implanted subcutaneously in immunodeficient mice and acts as a preferential metastatic site for intracardiacally injected human cancer cells. In these studies, microCT can still be used to analyze changes in the implant structure during bone metastasis progression (Rosol et al., 2003). Thus, microCT scanning can be used to study the interaction between metastatic cancer and bone during the development and progression of metastases.

2.2 MicroCT in metastatic cancer-bone interactions

As cancer progresses, metastasis occurs. Many cancers can metastasize to bone; however, metastatic multiple myelomas, breast carcinomas and prostate carcinomas, show a particular preference for the bone microenvironment. MicroCT has been used extensively to examine the interaction between metastatic tumors and the bone in both patient biopsies and animal models. Patient biopsies from bone bearing metastatic breast carcinomas, prostate carcinomas, or myelomas were analyzed by microCT to determine changes in the bone architecture, which could be used to diagnose malignancy. MicroCT scanning of metastatic biopsies was demonstrated to be quick and accurate in assessing excess bone turnover due to either increased resorption or formation due to malignant growth (Chappard et al., 2010). While the use of microCT to diagnose patient metastases is significant, a majority of published studies focus on the use of microCT to determine the factors responsible for the metastasis of primary cancers to bone using animal models (Table 2).

Model Types	Injection Sites	Bone Phenotypes
Spontaneous Syngeneic Xenograft Chemical Transgenic Reconstitution	Subcutaneous Intracardiac Intratibial Tail vein Orthotopic	Osteoblastic Osteoclastic Combination

Table 2. Animal models used in bone metastasis research. The different models, injection sites, and possible resulting bone phenotypes are listed. These diverse methods to trigger bone metastasis have had various rates of success and resulted in distinct bone phenotypes.

2.2.1 Multiple myelomas

Multiple myelomas are associated with osteolysis of the bone, which can be measured using microCT. In patients, microCT is used to measure changes in trabecular BV, as well as to visualize cortical lesions in three dimensions. In addition, microCT can be used to scan for metastatic myeloma lesions, which cause a derangement in the bone architecture. Mouse models of multiple myelomas have been established and are used to determine the consequences of malignant growth on the bone microenvironment. Using microCT, metastatic tumor lesion locations and the subsequent changes in the bone structure were accurately measured (Fowler et al., 2009; Postnov et al., 2009). Using these models, multiple myeloma lesions in the bone have been characterized as osteolytic, with a high number of

lesions in the cortical bone, leading to decreased trabecular BV/TV (Fowler et al., 2009). This model may be used for further studies of multiple myeloma metastases.

2.2.2 Breast cancer

Breast cancer bone metastases occur in 80% of patients with advanced disease and are predominantly osteolytic. MicroCT has been used successfully on patient biopsies to study treatment efficacies and to measure metastatic progression resulting in osteolysis. Correspondingly, microCT has been used to measure osteolysis during metastatic tumor growth in several breast cancer small animal models. When malignant breast carcinoma cells were injected into the femur of rats, decreases in trabecular and cortical bone mineral content were measured by microCT. Further, BV/TV, Tb.N, and Tb.Th were lower in limbs of mice with metastatic breast cancer (Kurth & Muller, 2001). In addition, several chemical agents can induce breast cancer in mice and rats. After rats were injected with N-methyl-N-nitrosourea to induce breast cancer, microCT was used to measure changes in the bone structure in a model of spontaneous cancer formation. Bone health was decreased in animals that developed tumors and both Tb.N and Tb.Th were decreased compared with control rats (Thorpe et al., 2010). These studies demonstrate that microCT imaging can be used to examine alterations in the bone architecture in response to metastatic breast cancer and to test the effectiveness of treatments to prevent tumor-induced osteolysis.

2.2.3 Prostate cancer

Prostate cancer metastasizing to the bone often results in osteoblastic lesions or a combination of osteoclastic and osteoblastic lesions. By comparing normal human bone tissue, osteosclerotic tissue, and osteoblastic metastatic lesions using microCT *ex vivo*, prostate cancer metastasis was shown to increase Tb.N and connectivity compared with benign osteosclerosis, but these lesions were found to have decreased BMD compared with normal and benign tissues (Sone et al., 2004). Prostate cancer metastasis is studied *in vivo* using rat, mouse, and dog models. While some instances of spontaneous prostate cancer exist in these models, a majority of prostate cancers are injected. Murine models of prostate cancer can be syngeneic in immunocompetent mice or xenograft models in immunocompromised mice, as well as a few spontaneous tumor models. Metastatic tumors in mice are largely osteolytic or a combination of osteoblastic and osteolytic (Singh & Figg, 2005). Using microCT, intratibial injections of prostate cancer cells was shown to result in extensive osteolysis of the trabeculae, followed by periosteal bone deposition (McCabe et al., 2008). By scanning the same region of bone over time, the rate of osteolysis can be measured and used to approximate the kinetics of tumor growth. The use of transgenic mice has also led to the identification of various proteins and genes involved in metastatic progression and initiation. Using transgenic mice, several bone proteins, including SPARC, were demonstrated to play important roles in the progression of metastatic prostate cancer lesions. A loss of SPARC protein resulted in enhanced osteolysis upon tumor challenge, as demonstrated by decreased BV/TV, Tb.Th, Tb.N, and BSA measured using microCT (McCabe et al., 2011). Also using microCT, this osteolysis was shown to be specific for prostate cancer, as intratibial injection of melanoma cells did not produce the same effect (McCabe et al., 2011). These studies underscore the importance of microCT scanning as a tool to measure bone structural indices during bone metastasis.

3. Primary tumor growth stimulates bone turnover

While prostate cancer metastases are osteoblastic, patients without visible metastases experience abnormal bone formation and resorption (Kingsley et al., 2007). Interestingly, prostate cancer cells are more likely to colonize bone during the remodelling period (Gomes et al., 2009); thus, it would benefit the tumor to stimulate bone turnover prior to metastasis. Although alterations in bone remodelling in patients with distant, primary cancers have been described, the mechanisms behind this pre-metastatic bone turnover have not been elucidated. Having previously established that intratibial injection of prostate cancer cells stimulates osteolysis (McCabe et al., 2008; McCabe et al., 2011), we wanted to determine the effects of primary tumor growth on the bone microenvironment. We used subcutaneous injections of prostate cancer cells to simulate a primary tumor and performed microCT scanning to assess changes in the bone structure.

3.1 Basic methods and considerations

The design of microCT experiments to study bone metastasis in small animals requires the consideration of various factors. The species, the age, the anesthetization of animals, the number of cells injected, and the time of tumor growth must be optimized prior to beginning experimentation. Further, several parameters of the microCT scanning procedure must be considered when planning experiments. Once these parameters have been optimized, as described below, microCT scanning of animals bearing tumors can be performed with both consistency and precision. Guidelines for microCT image acquisition and reporting of results were recently published (Bouxsein et al., 2010) and should be considered when designing experiments.

3.1.1 Animals

When planning microCT experiments, the choice of small animal must first be made. Most commonly, mice or rats are used in microCT experiments. The availability of a variety of transgenic mice results in their being highly used as experimental subjects. In mice, significant age-related trabecular bone loss begins by 24 weeks of age, and this must be accounted for when choosing animals. In addition, some variations in bone structure occur seasonally (Delahunty et al., 2009). Performing microCT scanning prior to tumor implantation or other intervention diminishes the seasonal and age-related alterations in bone architecture.

In our study, the mice used were six- to twelve-week-old and sex- and age-matched immunocompetent C57BL/6 (WT) or immunodeficient NOD/SCID mice (Jackson Laboratories, Bar Harbor, ME). All animal procedures were performed in accordance with an approved institutional protocol according to the guidelines of the Institutional Animal Care and Use Committee of the Cleveland Clinic.

3.1.2 Tumor injections

When preparing for tumor injections, the number of cells to be implanted and the time of growth vary by tumor type. The aggressiveness of the tumor cells or the cancer type can affect the rates of cell growth. In a previous study, we demonstrated the efficacy of different injections and injected cell numbers on the development of bone metastases (McCabe et al., 2008). In addition, we have found that murine melanoma cells must be injected in higher

numbers than murine prostate cancers to grow equally (Feng et al., 2011). Further, the use of xenograft models in immunodeficient animals results in diminished cell growth and longer incubation times necessary to obtain similarly sized tumors as those from syngeneic models. We have found that while human prostate cancers and murine prostate cancers can be injected at the same cell density, human prostate cancers require at least an extra week of growth to form palpable tumors (Feng et al., 2011). The main factor regulating cancer cell growth in mice is the health of the cells prior to implantation. Healthy cells below confluence will grow more readily than highly confluent cells. Thus, optimization must be performed to determine the best conditions for tumor cell growth and implantation.

In this study, cells are implanted subcutaneously with microCT scanning performed a day before injection. WT mice were injected subcutaneously (s.c.) with $4x10^5$ RM1 murine prostate cancer cells and sacrificed 12 days post implantation (5 mice/group). Separately, NOD/SCID mice were injected s.c. with $4x10^5$ LNCaP-C4-2 (C4-2) human prostate cancer cells and sacrificed 20 days post implantation (5 mice/group).

3.1.3 MicroCT scanning

The microCT scanning process requires several parameters to be optimized before scanning: the amount and type of anesthesia and restraint, the effects of ionizing radiation dosing, and the variables affecting repeated image acquisition. To obtain clear scans, mice must be restrained and/or anesthetized. Insufficient anesthesia can result in the subject moving during scanning, while excessive anesthesia can result in death (Paulus et al., 2001). When planning repeated scans, the effect of ionizing radiation dosing should be considered. Ionizing radiation doses can affect bone growth and may also affect tumors. A single scan produces radiation doses approximately 5% of the LD_{50} for mature mice (Paulus et al., 2001). However, repeated scans could result in changes in the tumor growth or bone resorption kinetics. To minimize the dosing effects, microCT scanning should be done at a specific interval. When performing repeated microCT scanning, several factors must be optimized to minimize differences between scans. Repeated image acquisition requires special considerations including positioning, scanning medium (for *ex vivo*), image resolution, and uniform regions of interest (Stock, 2009). During processing, samples are filtered, segmented, registered, and uniform regions of interest are applied to create masks for differentiating between cortical and trabecular bone. Phantom calibration must be performed regularly to calibrate the scanner values for the measurement of morphometric parameters. Phantom values are calculated for materials whose dimensions and geometries are known (Stoico et al., 2010). For bone research, values are measured using phantoms for air, water, and bone. The registering of bones results in increased reproducibility between scans and is necessary to measure changes in the bone structure across different time points (Nishiyama et al., 2010). By optimizing all of these scanning parameters, changes in the bone structure can be measured and registered over time.

In our study, mice are anesthetized by i.p. injection of 100 mg/kg ketamine and 10 mg/kg xylazine prior to cell implantation and microCT scanning. MicroCT analysis of the proximal tibiae was performed one day prior to cell implantation, 3 days later, and then every 7 days until experimental termination to minimize the effects of multiple radiation doses. Scans were conducted in the Cleveland Clinic Biomedical Imaging and Analysis Core Center on a GE eXplore Locus microCT (GE Healthcare, Piscataway, NJ) and 360 X-ray projections were collected in 1^o increments (80 kVp; 500 mA; 26 min total scan time). Projection images were

preprocessed and reconstructed into 3-dimensional volumes (1024^3 voxels, 20 μm resolution) on a 4PC reconstruction cluster using a modified tent-FDK cone-beam algorithm (GE reconstruction software). Three-dimensional data was processed and rendered (isosurface/maximum intensity projections) using MicroView (GE Healthcare). For each volume, a plane perpendicular to the z-axis/tibial shaft was generated and placed at the base of the growth plate. A second, parallel plane was defined 1.0 mm below and the entire volume was cropped to this volume of interest for quantitative analysis. Image stacks from each volume of interest were exported for quantitative analysis. Cancellous bone masks were generated in MicroView and 3D trabecular structural indices were extracted using custom MatLab (The MathWorks, Inc, Natick, MA) algorithms. Tb.Th and Tb.Sp were determined by previously reported methods (Hildebrand et al., 1999). Tb.N was calculated by taking the inverse of the average distance between the medial axes of trabecular bone segments. BV/TV (total bone voxels divided by total cancellous bone mask voxels) and BSA (sum of pixels along edges of trabecular bone) were also calculated for each VOI. Phantom calibrations are perfomed regularly using air, water, and bone phantoms.

3.2 Representative results and discussion

Using subcutaneous tumor implantation and microCT scanning, we assessed the consequences of primary tumor growth on bone metabolism. We found that injection of murine prostate cancer cells (RM1) in immunocompetent mice results in enhanced bone formation compared with sham injected mice after 12 days of tumor growth. Reconstructions of the microCT scanned bones demonstrate increased trabecular bone in RM1 injected mice (Figure 1). When changes in the bone structural indices were quantified,

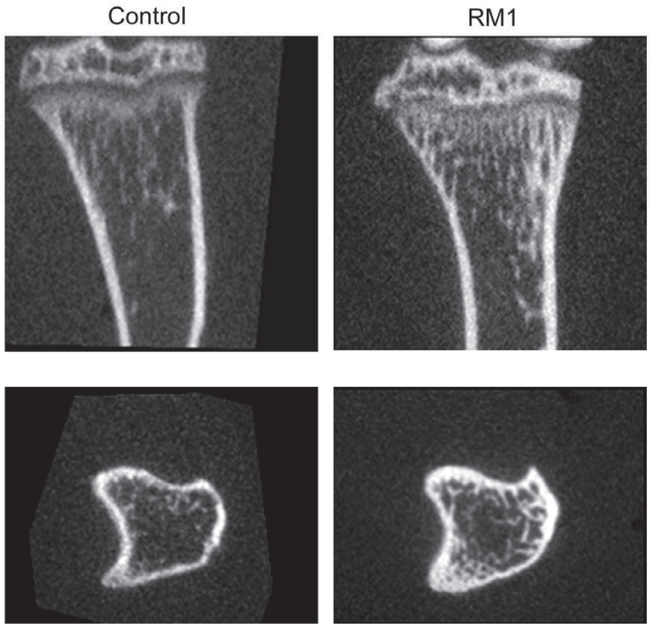

Fig. 1. Reconstructions of microCT scanned bones. Immunocompetent mice were injected with $4x10^5$ murine prostate cancer cells (RM1) or mock injected (Control). Both frontal (top) and transverse planes (bottom) are shown of the proximal tibia.

we found that BV/TV was increased 1.79 fold in mice bearing tumors (Figure 2A). In addition, BSA increased 1.58 fold, demonstrating an overall stimulation of bone formation (Figure 2A). Tb.Th was found to be 1.37 fold higher in mice bearing tumors, with a corresponding 0.72 fold decrease in Tb.Sp. Tb.N did not change significantly during tumor growth (Figure 2B). Thus, bone formation occurred through remodelling of the existing trabeculae and not *de novo* bone formation.

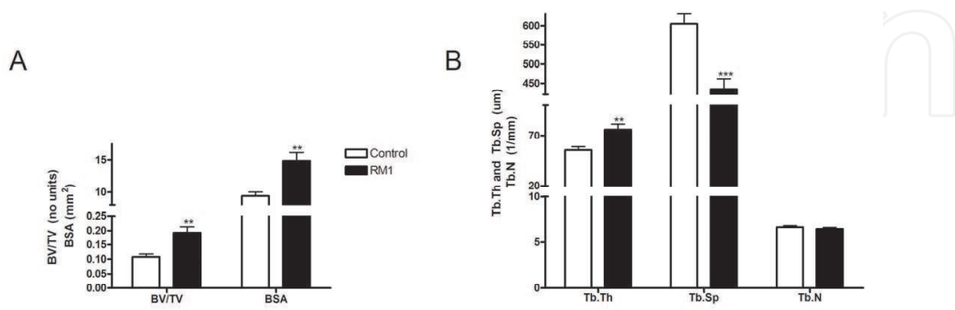

Fig. 2. Bone formation is enhanced in mice bearing prostate cancer tumors.
Immunocompetent mice were injected with $4x10^5$ murine prostate cancer cells (RM1; black bars) or mock injected (Control; white bars). (A) MicroCT scanning was performed after 12 days of tumor growth and bone volume to total volume ratio (BV/TV) and bone surface area (BSA) were measured to assess overall volume changes. (B) Trabecular indices were analyzed by microCT and trabecular thickness (Tb.Th), trabecular spacing (Tb.Sp), and trabecular number (Tb.N) were quantified. Measurements are represented as mean ± S.E.M. ** represents $p<0.01$ and *** represents $p<0.001$ by Student's *t* test vs. control.

We next used a xenograft model to determine whether these findings were specific to RM1 cells. Injection of human prostate cancer cells subcutaneously in immunodeficient mice demonstrated similarly increased bone formation. MicroCT scanning was performed 4, 11, and 18 days after tumor implantation to assess changes in the bone architecture over time. Reconstructions exhibit the changes in trabecular structure between days 11 and 18 (Figure 3).

Quantification of changes in bone structural indices demonstrated that significant bone formation occurs between 4 and 11 days of tumor growth, followed by a compensatory decrease around day 18. BV/TV was 0.94 fold of control on day 4, 1.27 fold higher on day 11, and 0.46 fold lower on day 18 compared with mice without tumors (Figure 4A). Further, BSA values of injected mice compared with control were 1.05 fold on day 4, 1.11 fold on day 11, and 0.55 fold on day 18 (Figure 4B). Thus, the overall amount of bone increases between days 4 and 11, then begins to decrease by day 18.

To determine if the trabecular bone remodelling was responsible for these changes in BV and BSA, the structural indices of the trabecular bone were quantified. Tb.Th was increased 1.16 fold on day 11 and decreased 0.70 fold on day 18, while Tb.Sp demonstrated corresponding changes of 0.82 fold on day 11 and 2.87 fold on day 18 compared with control (Figure 5 A and B). Tb.N remained unchanged over the time course (Figure 5C). Thus, subcutaneous tumor growth stimulates bone formation initially, with later compensatory bone destruction as the enhanced osteoblast proliferation and function stimulates osteoclast activity.

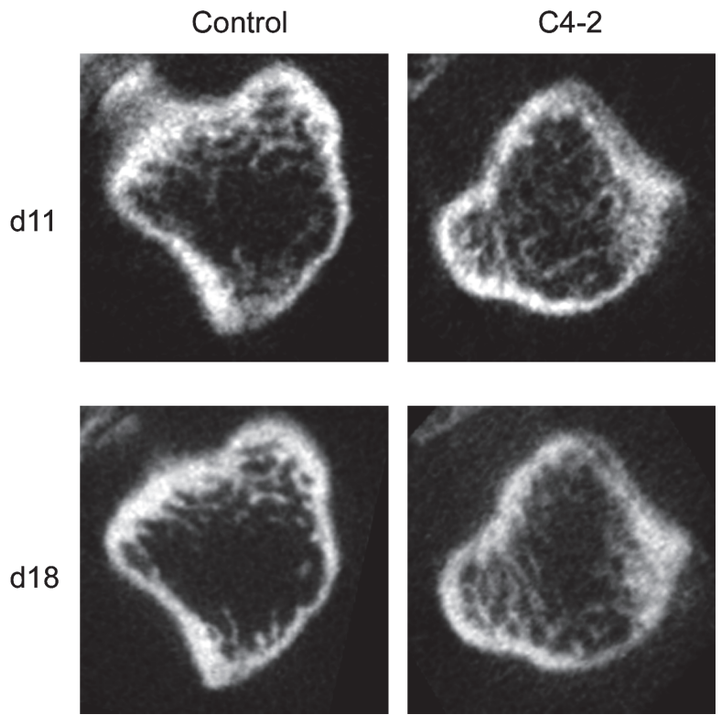

Fig. 3. Reconstructions of the microCT scanned bones. Immunodeficient mice were injected with $4x10^5$ human prostate cancer cells subcutaneously (C4-2) or mock injected (Control). Both frontal and transverse planes are shown of the proximal tibia from scans completed on days (d) 11 and 18.

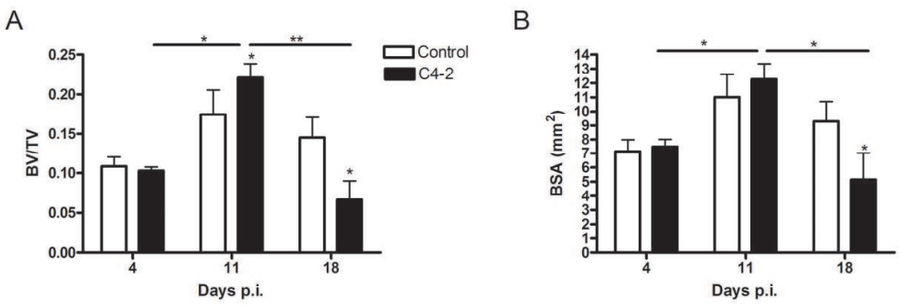

Fig. 4. Implantation of human prostate cancer in immunodeficient mice results in initial bone formation followed by bone resorption. Human prostate cancer cells ($4x10^5$ cells/side) (C4-2; black columns) were injected or a mock injection was performed (Control; white columns). MicroCT scanning was used to quantify bone volume to total volume ratio (BV/TV; A) or bone surface area (BSA; B). Measurements are represented as mean ± S.E.M. * represents $p<0.05$ and ** represents $p<0.01$ by one-way ANOVA (between time points) or Student's *t* test (vs. Control).

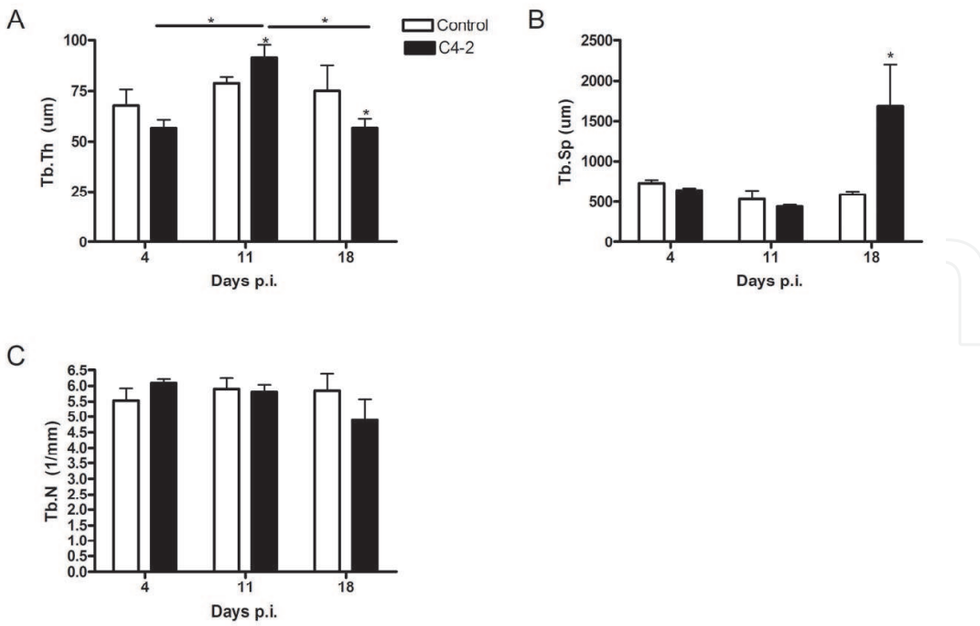

Fig. 5. Subcutaneous human tumor implantation stimulates changes in trabecular bone architecture. Human prostate cancer cells ($4x10^5$ cells/side) (C4-2; black columns) were injected or a mock injection was performed (Control; white columns). MicroCT scanning was used to quantify trabecular thickness (Tb.Th; A), trabecular spacing (Tb.Sp; B), and trabecular number (Tb.N; C). Measurements are represented as mean ± S.E.M. * represents $p<0.05$ by one-way ANOVA (between time points) or Student's *t* test (vs. Control).

Our data demonstrate that primary tumor growth stimulates bone formation, possibly followed later by compensatory bone resorption. This increase in bone formation is similar to that seen in prostate cancer patients (Kingsley et al., 2007). Stimulation of bone remodelling may result in the release of growth factors and cytokines capable of promoting tumor growth. Several cytokines known to be sequestered within the bone matrix or produced by osteoblasts, including transforming growth factor β1, receptor activator of NF-κB ligand, and osteopontin, are capable of promoting tumor growth. In addition, bone turnover may induce the release of bone marrow-progenitor cells into the circulation (Lymperi et al., 2011). We have shown that these progenitors are recruited into tumors supporting angiogenesis and continued tumor growth (Feng et al., 2011). The enhanced bone remodelling may also function to prepare the microenvironment for the future invasion of the metastatic tumor. We have previously shown that tumors secrete into the circulation several cytokines which may be promoting bone remodelling (Kerr et al., 2010), demonstrating a possible direct link between the tumor and the induced bone turnover. Thus, our studies demonstrate the importance of microCT as a tool to examine the bone structure in bone metastasis research.

4. Future of microCT in cancer bone metastasis research

The dominant microCT systems currently used are desktop microCT machines which focus mainly on the microstructural level. Newer machines using synchrotron radiation microCT

and nanoCT provide higher resolution images and may provide more precise measurements of bone structure indices. Further, combining microCT with PET or bioluminescence will result in the improved imaging of tumors within the bone microenvironment. Improved imaging of both the bone and tumor at the cellular level promotes the use of these technologies in metastatic signaling and micrometastasis, as well as the testing of various therapeutic target efficacies.

4.1 NanoCT

While the dominant desktop microCT systems available provide resolutions between 5-100 μm, third-generation synchrotron radiation systems have resolutions below 1 μm. These resolutions down to 100 nm are called nanoCT and may allow for imaging on the cellular level including the canal network, osteocyte lacunae, and even single cells. In addition, these machines can be used in the visualization of microfractures (Muller, 2009; Stock, 2009). A recent study used nanoCT to examine osteocyte lacunae and the canalicular network (Dierolf et al., 2010). Analysis of scans from nanoCT machines will provide increased precision of measurements and improved quantification of early changes in the bone structure due to osteoporosis or therapeutic treatments. Until the development of nanoCT systems is completed and the systems become widely available, desktop microCT systems alone or in combination with other imaging systems will remain the main tool for analysis of the bone structure.

4.2 Combined imaging techniques

A recent trend in microCT imaging has been the development of PET-CTs, which allow simultaneous PET and CT scanning. Using this machine, overlays of low resolution tumors with high resolution microCT scans can be produced (Schambach et al., 2010). Further, fusion of bioluminescent imaging with microCT would allow for improved visualization of tumor cells along the bone and of local changes in bone cells and architecture. Bioluminescent imaging requires the use of luciferase reporters to be expressed by the tumor cells and results in a strong signal without any requirement for external illumination. In addition, fluorescent proteins or dots can be introduced to cells prior to implantation (de Boer et al., 2006; Henriquez et al., 2007). The use of bioluminescent imaging with microCT was recently used to measure the kinetics of intraosseous tumor growth, resultant bone destruction, and correlations between the two over time (Fritz et al., 2007). In addition, luciferase can be introduced to osteoblasts or osteoclasts to monitor their activity, proliferation, and migration along the bone during metastatic tumor growth or in response to pre-metastatic signals from a primary tumor. Finally, luciferase activity can be used to monitor inflammation, angiogenesis, apoptosis, or signal transduction in metastatic tumors within the bone microenvironment and their association with altered bone architecture (de Boer et al., 2006). PET-CT or bioluminescent imaging, when combined with microCT, will permit visualization of micrometastases and metastatic soft tumors in the bone microenvironment.

4.3 Metastatic signaling

MicroCT scanning can also be used to study the proteins and signaling cascades involved in inducing bone changes during the metastatic process. The mechanisms of primary

cancer metastasis to bone are still being elucidated, although several proteins and signaling cascades have been shown to play important roles in bone metastasis. For example, the $\alpha_v\beta_3$ integrin on prostate cancer cells is necessary for the progression of metastatic growth in bone. Further, this integrin is responsible for increases in bone formation caused by metastatic prostate cancer visualized by microCT scanning (McCabe et al., 2007). Building upon this study, the importance of extracellular proteins recognized by the $\alpha_v\beta_3$ integrin in prostate cancer progression has been studied using microCT and transgenic mice (McCabe et al., 2011). Using transgenic mice or cancer cells with proteins over-expressed or knocked-down, the signals regulating the metastasis of prostate cancer to bone can be examined using microCT to repeatedly and non-invasively study the bone structure.

4.4 Treatment efficacies

The efficacy of therapeutics can be measured using *ex vivo* microCT scanning of human biopsies or *in vivo* scanning of small animals. MicroCT imaging alone can be used on biopsies or animals to determine the effectiveness of drugs in altering the bone microenvironment. Therapies aimed at improving bone density or trabecular thickness can easily be measured and may be used in studies of osteoporosis and osteogenesis imperfecta. MicroCT scanning of biopsies can also be used to assess changes in primary osteosarcoma tumor structure and size. For metastatic soft tumors, a combination of microCT and optical imaging techniques are most useful in analyzing therapeutic effectiveness on shrinking tumors and maintaining the bone architecture. This non-invasive testing allows for the continuous monitoring of tumors during their growth or remission (Henriquez et al., 2007). MicroCT scanning has been used to study the effectiveness of treatments designed to slow down the progression of osteolysis during bone metastasis progression. In a small animal model, zolendronic acid treatment decreased bone resorption as shown by microCT scanning (Johnson et al., 2011). In another study, an osteoprotegrin-producing adenovirus was demonstrated to result in increased BV/TV and connectivity and thus, was shown to protect against metastatic bone loss (Chanda et al., 2008). Further, the main symptom resulting from bone metastases is pain, which is the major factor responsible for decreased quality of life. Intraosseous tumor implantation and microCT scanning were used to study the correlation of bone pain with bone destruction in a rat model (Dore-Savard et al., 2010). This model can be used in the future to examine the effectiveness of therapeutics targeting bone pain. In summary, microCT imaging can be used to determine the efficacy of treatments in altering the bone architecture in a variety of diseases.

5. Conclusion

The development of microCT scanners provided a means for analyzing the bone structure and mineralization level non-destructively. MicroCT alone provides quantitative and qualitative scanning at a high sensitivity and micrometer resolution, with newer imaging systems providing even nanometer resolutions. These machines have allowed for extensive research on bone and bone metastasis to be completed. Current studies are using microCT scanning to elucidate the mechanisms behind cancer metastasis and to determine the effectiveness of treatments. Using the basic procedures and considerations when planning microCT scanning experiments discussed, consistency and precision can be achieved in repeated scans of small animals. The data presented here establish the usefulness of

microCT scanning to measure pre-metastatic bone changes. Our data demonstrate that primary tumors communicate with the bone microenvironment prior to metastasis stimulating bone formation in two tumor models. Using microCT imaging alone or in combination with other methodologies will permit continued examination of the metastatic process. Combined imaging techniques and advances in microCT systems will allow for continued research on metastatic signaling, metastatic tumor development and progression, and therapeutic efficacies. Thus, microCT has been come an essential tool in bone metastasis research.

6. Acknowledgment

We would like to thank Dr. Amit Vasanji, who developed the software and analysis techniques for our microCT analysis, and Rick Rozic for technical assistance with the microCT scanner. We also thank Miroslava Tischenko for her assistance with the mouse colony. B.A.K. was supported by a Ruth L. Kirschstein NRSA award (F32 CA142133) from the NIH/NCI. This study was supported by research funding from the NIH/NCI grant (CA126847) to T.V.B.

7. References

Adams, C. S., V. Antoci, Jr., G. Harrison, P. Patal, T. A. Freeman, I. M. Shapiro, J. Parvizi, N. J. Hickok, S. Radin & P. Ducheyne. (2009). Controlled release of vancomycin from thin sol-gel films on implant surfaces successfully controls osteomyelitis. *J Orthop Res*, Vol. 27, No. 6, pp. 701-709. ISSN 1554-527X

Bouxsein, M. L., S. K. Boyd, B. A. Christiansen, R. E. Guldberg, K. J. Jepsen & R. Muller. (2010). Guidelines for assessment of bone microstructure in rodents using micro-computed tomography. *J Bone Miner Res*, Vol. 25, No. 7, pp. 1468-1486. ISSN 1523-4681

Chanda, D., T. Isayeva, S. Kumar, G. P. Siegal, A. A. Szafran, K. R. Zinn, V. V. Reddy & S. Ponnazhagan. (2008). Systemic osteoprotegerin gene therapy restores tumor-induced bone loss in a therapeutic model of breast cancer bone metastasis. *Mol Ther*, Vol. 16, No. 5, pp. 871-878. ISSN 1525-0024

Chappard, D., H. Libouban, E. Legrand, N. Ifrah, C. Masson, M. F. Basle & M. Audran. (2010). Computed microtomography of bone specimens for rapid analysis of bone changes associated with malignancy. *Anat Rec (Hoboken)*, Vol. 293, No. 7, pp. 1125-1133. ISSN 1932-8494

de Boer, J., C. van Blitterswijk & C. Lowik. (2006). Bioluminescent imaging: emerging technology for non-invasive imaging of bone tissue engineering. *Biomaterials*, Vol. 27, No. 9, pp. 1851-1858. ISSN 0142-9612

Delahunty, K. M., L. G. Horton, H. F. Coombs, 3rd, K. L. Shultz, K. L. Svenson, M. A. Marion, M. F. Holick, W. G. Beamer & C. J. Rosen. (2009). Gender- and compartment-specific bone loss in C57BL/6J mice: correlation to season? *J Clin Densitom*, Vol. 12, No. 1, pp. 89-94. ISSN 1094-6950

Dierolf, M., A. Menzel, P. Thibault, P. Schneider, C. M. Kewish, R. Wepf, O. Bunk & F. Pfeiffer. (2010). Ptychographic X-ray computed tomography at the nanoscale. *Nature*, Vol. 467, pp. 436-9. ISSN 0028-0836

Dore-Savard, L., V. Otis, K. Belleville, M. Lemire, M. Archambault, L. Tremblay, J. F. Beaudoin, N. Beaudet, R. Lecomte, M. Lepage, L. Gendron & P. Sarret. (2010). Behavioral, medical imaging and histopathological features of a new rat model of bone cancer pain. *PLoS One*, Vol. 5, No. 10, pp. e13774. ISSN 1932-6203

Feng, W., M. Madajka, B. A. Kerr, G. H. Mahabeleshwar, S. W. Whiteheart & T. V. Byzova. (2011). A novel role for platelet secretion in angiogenesis: mediating bone marrow-derived cell mobilization and homing. *Blood*, Vol. 117, No. 14, pp. 3893-902. ISSN 1528-0020

Fowler, J. A., G. R. Mundy, S. T. Lwin, C. C. Lynch & C. M. Edwards. (2009). A murine model of myeloma that allows genetic manipulation of the host microenvironment. *Dis Model Mech*, Vol. 2, No. 11-12, pp. 604-611. ISSN 1754-8411

Freeman, T. A., P. Patel, J. Parvizi, V. Antoci, Jr. & I. M. Shapiro. (2009). Micro-CT analysis with multiple thresholds allows detection of bone formation and resorption during ultrasound-treated fracture healing. *J Orthop Res*, Vol. 27, No. 5, pp. 673-679. ISSN 1554-527X

Fritz, V., P. Louis-Plence, F. Apparailly, D. Noel, R. Voide, A. Pillon, J. C. Nicolas, R. Muller & C. Jorgensen. (2007). Micro-CT combined with bioluminescence imaging: a dynamic approach to detect early tumor-bone interaction in a tumor osteolysis murine model. *Bone*, Vol. 40, No. 4, pp. 1032-1040. ISSN 8756-3282

Genant, H. K., K. Engelke & S. Prevrhal. (2008). Advanced CT bone imaging in osteoporosis. *Rheumatology (Oxford)*, Vol. 47 Suppl 4, pp. iv9-16. ISSN 1462-0332

Gielkens, P. F., J. Schortinghuis, J. R. de Jong, M. C. Huysmans, M. B. Leeuwen, G. M. Raghoebar, R. R. Bos & B. Stegenga. (2008). A comparison of micro-CT, microradiography and histomorphometry in bone research. *Arch Oral Biol*, Vol. 53, No. 6, pp. 558-566. ISSN 0003-9969

Gomes, R. R., Jr., P. Buttke, E. M. Paul & R. A. Sikes. (2009). Osteosclerotic prostate cancer metastasis to murine bone are enhanced with increased bone formation. *Clin Exp Metastasis*, Vol. 26, No. 7, pp. 641-651. ISSN 1573-7276

Henriquez, N. V., P. G. van Overveld, I. Que, J. T. Buijs, R. Bachelier, E. L. Kaijzel, C. W. Lowik, P. Clezardin & G. van der Pluijm. (2007). Advances in optical imaging and novel model systems for cancer metastasis research. *Clin Exp Metastasis*, Vol. 24, No. 8, pp. 699-705. ISSN 0262-0898

Hildebrand, T., A. Laib, R. Muller, J. Dequeker & P. Ruegsegger. (1999). Direct three-dimensional morphometric analysis of human cancellous bone: microstructural data from spine, femur, iliac crest, and calcaneus. *J Bone Miner Res*, Vol. 14, No. 7, pp. 1167-1174. ISSN 0884-0431

Jiang, Y., J. Zhao, D. L. White & H. K. Genant. (2000). Micro CT and Micro MR imaging of 3D architecture of animal skeleton. *J Musculoskelet Neuronal Interact*, Vol. 1, No. 1, pp. 45-51. ISSN 1108-7161

Johnson, L. C., R. W. Johnson, S. A. Munoz, G. R. Mundy, T. E. Peterson & J. A. Sterling. (2011). Longitudinal live animal microCT allows for quantitative analysis of tumor-induced bone destruction. *Bone*, pp. ISSN 1873-2763

Jones, J. R., R. C. Atwood, G. Poologasundarampillai, S. Yue & P. D. Lee. (2009). Quantifying the 3D macrostructure of tissue scaffolds. *J Mater Sci Mater Med*, Vol. 20, No. 2, pp. 463-471. ISSN 0957-4530

Kerr, B. A., R. Miocinovic, A. K. Smith, E. A. Klein & T. V. Byzova. (2010). Comparison of tumor and microenvironment secretomes in plasma and in platelets during prostate cancer growth in a xenograft model. *Neoplasia*, Vol. 12, No. 5, pp. 388-396. ISSN 1476-5586

Kingsley, L. A., P. G. Fournier, J. M. Chirgwin & T. A. Guise. (2007). Molecular biology of bone metastasis. *Mol Cancer Ther*, Vol. 6, No. 10, pp. 2609-2617. ISSN 1535-7163

Kurth, A. A. & R. Muller. (2001). The effect of an osteolytic tumor on the three-dimensional trabecular bone morphology in an animal model. *Skeletal Radiol*, Vol. 30, No. 2, pp. 94-98. ISSN 0364-2348

Laib, A., O. Barou, L. Vico, M. H. Lafage-Proust, C. Alexandre & P. Rugsegger. (2000). 3D micro-computed tomography of trabecular and cortical bone architecture with application to a rat model of immobilisation osteoporosis. *Med Biol Eng Comput*, Vol. 38, No. 3, pp. 326-332. ISSN 0140-0118

Langheinrich, A. C., C. Stolle, M. Kampschulte, D. Lommel, W. S. Rau & B. Bassaly. (2008). Diagnostic value of ex-vivo three-dimensional micro-computed tomography imaging of primary nonhematopoietic human bone tumors: osteosarcoma versus chondrosarcoma. *Acta Radiol*, Vol. 49, No. 8, pp. 940-948. ISSN 1600-0455

Lymperi, S., A. Ersek, F. Ferraro, F. Dazzi & N. J. Horwood. (2011). Inhibition of osteoclast function reduces hematopoietic stem cell numbers in vivo. *Blood*, Vol. 117, No. 5, pp. 1540-1549. ISSN 1528-0020

Martin-Badosa, E., A. Elmoutaouakkil, S. Nuzzo, D. Amblard, L. Vico & F. Peyrin. (2003). A method for the automatic characterization of bone architecture in 3D mice microtomographic images. *Comput Med Imaging Graph*, Vol. 27, No. 6, pp. 447-458. ISSN 0895-6111

Mayer-Kuckuk, P. & A. L. Boskey. (2006). Molecular imaging promotes progress in orthopedic research. *Bone*, Vol. 39, No. 5, pp. 965-977. ISSN 8756-3282

McCabe, N. P., S. De, A. Vasanji, J. Brainard & T. V. Byzova. (2007). Prostate cancer specific integrin alphavbeta3 modulates bone metastatic growth and tissue remodeling. *Oncogene*, Vol. 26, No. 42, pp. 6238-6243. ISSN 0950-9232

McCabe, N. P., M. Madajka, A. Vasanji & T. V. Byzova. (2008). Intraosseous injection of RM1 murine prostate cancer cells promotes rapid osteolysis and periosteal bone deposition. *Clin Exp Metastasis*, Vol. 25, No. 5, pp. 581-590. ISSN 0262-0898

McCabe, N. P., B. A. Kerr, M. Madajka, A. Vasanji & T. V. Byzova. (2011). Augmented Osteolysis in SPARC-Deficient Mice with Bone-Residing Prostate Cancer. *Neoplasia*, Vol. 13, No. 1, pp. 31-39. ISSN 1476-5586

Muller, R. (2009). Hierarchical microimaging of bone structure and function. *Nat Rev Rheumatol*, Vol. 5, No. 7, pp. 373-381. ISSN 1759-4804

Nishiyama, K. K., G. M. Campbell, R. J. Klinck & S. K. Boyd. (2010). Reproducibility of bone micro-architecture measurements in rodents by in vivo micro-computed tomography is maximized with three-dimensional image registration. *Bone*, Vol. 46, No. 1, pp. 155-161. ISSN 1873-2763

Paulus, M. J., S. S. Gleason, S. J. Kennel, P. R. Hunsicker & D. K. Johnson. (2000). High resolution X-ray computed tomography: an emerging tool for small animal cancer research. *Neoplasia*, Vol. 2, No. 1-2, pp. 62-70. ISSN 1522-8002

Paulus, M. J., S. S. Gleason, M. E. Easterly & C. J. Foltz. (2001). A review of high-resolution X-ray computed tomography and other imaging modalities for small animal research. *Lab Anim (NY)*, Vol. 30, No. 3, pp. 36-45. ISSN 0093-7355

Postnov, A. A., H. Rozemuller, V. Verwey, H. Lokhorst, N. De Clerck & A. C. Martens. (2009). Correlation of high-resolution X-ray micro-computed tomography with bioluminescence imaging of multiple myeloma growth in a xenograft mouse model. *Calcif Tissue Int*, Vol. 85, No. 5, pp. 434-443. ISSN 1432-0827

Ravoori, M., A. J. Czaplinska, C. Sikes, L. Han, E. M. Johnson, W. Qiao, C. Ng, D. D. Cody, W. A. Murphy, K. A. Do, N. M. Navone & V. Kundra. (2010). Quantification of mineralized bone response to prostate cancer by noninvasive in vivo microCT and non-destructive ex vivo microCT and DXA in a mouse model. *PLoS One*, Vol. 5, No. 3, pp. e9854. ISSN 1932-6203

Reynolds, D. G., S. Shaikh, M. O. Papuga, A. L. Lerner, R. J. O'Keefe, E. M. Schwarz & H. A. Awad. (2009). muCT-based measurement of cortical bone graft-to-host union. *J Bone Miner Res*, Vol. 24, No. 5, pp. 899-907. ISSN 1523-4681

Rolf, Z., H. Astrid, S. Franziska, R. Heinrich, K. C. James, S. Helmut & B. Christoph. (2010). High Resolution X-Ray Tomography- 3D Imaging for Tissue Engineering Applications, In: *Tissue Engineering*, D. Eberli. pp. 337-358, InTech. ISBN 978-953-307-079-7, Vienna, Austria

Rosol, T. J., S. H. Tannehill-Gregg, B. E. LeRoy, S. Mandl & C. H. Contag. (2003). Animal models of bone metastasis. *Cancer*, Vol. 97, No. 3 Suppl, pp. 748-757. ISSN 0008-543X

Ruegsegger, P., B. Koller & R. Muller. (1996). A microtomographic system for the nondestructive evaluation of bone architecture. *Calcif Tissue Int*, Vol. 58, No. 1, pp. 24-29. ISSN 0171-967X

Schambach, S. J., S. Bag, L. Schilling, C. Groden & M. A. Brockmann. (2010). Application of micro-CT in small animal imaging. *Methods*, Vol. 50, No. 1, pp. 2-13. ISSN 1095-9130

Singh, A. S. & W. D. Figg. (2005). In vivo models of prostate cancer metastasis to bone. *J Urol*, Vol. 174, No. 3, pp. 820-826. ISSN 0022-5347

Sone, T., T. Tamada, Y. Jo, H. Miyoshi & M. Fukunaga. (2004). Analysis of three-dimensional microarchitecture and degree of mineralization in bone metastases from prostate cancer using synchrotron microcomputed tomography. *Bone*, Vol. 35, No. 2, pp. 432-438. ISSN 8756-3282

Stock, S. R. (2009). *MicroComputed Tomography: Methodology and Applications* CRC Press, ISBN 978-1-4200-5876-5, Boca Raton

Stoico, R., S. Tassani, E. Perilli, F. Baruffaldi & M. Viceconti. (2010). Quality control protocol for in vitro micro-computed tomography. *J Microsc*, Vol. 238, No. 2, pp. 162-172. ISSN 1365-2818

Thorpe, M. P., R. J. Valentine, C. J. Moulton, A. J. Johnson, E. M. Evans & D. K. Layman. (2010). Breast tumors induced by N-methyl-N-nitrosourea are damaging to bone strength, structure and mineralization in the absence of metastasis in rats. *J Bone Miner Res*, pp. ISSN 1523-4681

Wazen, R. M., L. P. Lefebvre, E. Baril & A. Nanci. (2010). Initial evaluation of bone ingrowth into a novel porous titanium coating. *J Biomed Mater Res B Appl Biomater*, Vol. 94, No. 1, pp. 64-71. ISSN 1552-4981

Yang, S. Y., H. Yu, J. E. Krygier, P. H. Wooley & M. P. Mott. (2007). High VEGF with rapid growth and early metastasis in a mouse osteosarcoma model. *Sarcoma*, Vol. 2007, pp. 95628. ISSN 1357-714X

IntechOpen

IntechOpen

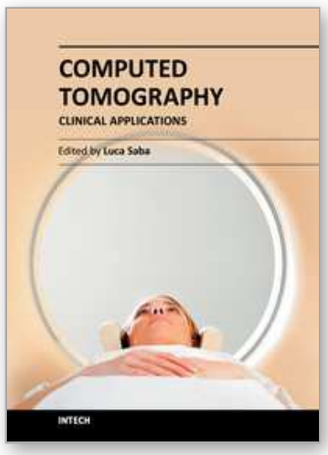

Computed Tomography - Clinical Applications
Edited by Dr. Luca Saba

ISBN 978-953-307-378-1
Hard cover, 342 pages
Publisher InTech
Published online 05, January, 2012
Published in print edition January, 2012

Computed Tomography (CT), and in particular multi-detector-row computed tomography (MDCT), is a powerful non-invasive imaging tool with a number of advantages over the others non- invasive imaging techniques. CT has evolved into an indispensable imaging method in clinical routine. It was the first method to non-invasively acquire images of the inside of the human body that were not biased by superimposition of distinct anatomical structures. The first generation of CT scanners developed in the 1970s and numerous innovations have improved the utility and application field of the CT, such as the introduction of helical systems that allowed the development of the "volumetric CT" concept. In this book we want to explore the applications of CT from medical imaging to other fields like physics, archeology and computer aided diagnosis. Recently interesting technical, anthropomorphic, forensic and archeological as well as paleontological applications of computed tomography have been developed. These applications further strengthen the method as a generic diagnostic tool for non- destructive material testing and three-dimensional visualization beyond its medical use.

How to reference
In order to correctly reference this scholarly work, feel free to copy and paste the following:

Bethany A. Kerr and Tatiana V. Byzova (2012). MicroCT: An Essential Tool in Bone Metastasis Research, Computed Tomography - Clinical Applications, Dr. Luca Saba (Ed.), ISBN: 978-953-307-378-1, InTech, Available from: http://www.intechopen.com/books/computed-tomography-clinical-applications/microct-an-essential-tool-in-bone-metastasis-research

INTECH
open science | open minds

InTech Europe
University Campus STeP Ri
Slavka Krautzeka 83/A
51000 Rijeka, Croatia
Phone: +385 (51) 770 447
Fax: +385 (51) 686 166
www.intechopen.com

InTech China
Unit 405, Office Block, Hotel Equatorial Shanghai
No.65, Yan An Road (West), Shanghai, 200040, China
中国上海市延安西路65号上海国际贵都大饭店办公楼405单元
Phone: +86-21-62489820
Fax: +86-21-62489821

© 2012 The Author(s). Licensee IntechOpen. This is an open access article distributed under the terms of the Creative Commons Attribution 3.0 License, which permits unrestricted use, distribution, and reproduction in any medium, provided the original work is properly cited.

IntechOpen

IntechOpen